ELSEVIER

Materials Chemistry and Physics 53 (1998) 243–246

MATERIALS CHEMISTRY AND PHYSICS

Materials Science Communication

Electronic behavior of Li–GIC in the lithium secondary battery

Yuan-Haun Lee [a,*], Wen-Ku Chang [a], Chun-Hsiung Fang [a], Yea-Fu Huang [b], Andy A. Wang [c]

[a] *Graduate Institute of Materials Science and Engineering, National Taiwan University, Taipei, Taiwan*
[b] *Department of Chemistry, Chung-yuan University, Chung Li, Taiwan*
[c] *Nan Ya-Junior College, Chung Li, Taiwan*

Received 30 December 1996; received in revised form 28 November 1997; accepted 28 November 1997

Abstract

Composite materials which, when mixing graphite with montmorillonite and TEF oligomer, can replace lithium metal as the negative electrode materials for the lithium secondary batteries have been studied. The anode composite materials were fabricated by mixing graphite with different components of montmorillonite and TFE oligomer, even lithium fluoride. The microstructure of the anodic composite materials were characterized by X-ray diffraction and its data was refined with the Rietveld analysis. The electric properties of the composite materials were characterized by electrochemical impedance spectroscopy (EIS). The electrochemical behaviours of the composite materials were investigated in a 1 M $LiPF_6$ solution with a 50:50 mixture of ethylene carbonate (EC) and diethylene carbonate (DEC). In our previous study, with the increased graphitization of the graphite materials, the layer structure became more orderly and the discharge capacity higher, however, the electronic behavior of Li–GIC, as a composite material mixed with montmorillonite intercalated by TEF oligomer, became complicated in this case. From the cyclic voltammetry, with the increasing of potential sweeping rate, the anodic peak would shift to the higher potential and show a larger current. The relationship between the component of anode composite materials and its intercalation as the result of the electrochemical behaviours will be discussed.

Keywords: Electronic behavior; Lithium secondary batteries

1. Introduction

In recent years, the graphitizating and non-graphitizating carbon materials such as natural graphites [1], artificial graphites [2], carbon black [3], actived carbon [4], pitch cokes [5], carbon fibers [6], mesocarbon [7] and carbonized polymers [8] were investigated for use as Li-intercalation negative electrodes for rechargeable lithium batteries. Those carbon anodes can avoid the formation of lithium dendrite on the surface and has particular advantages. Therefore, good reliability, high voltage, high capacity, little pollution and safety of the batteries can be obtained. However, there are still many works to be done. such as reducing irreversible capacity losses, choosing carbon materials with large capacity, and so on [9,10]. The main structural factors of the lattice parameters (a and c), graphitization degree and crystallite sizes (L_a and L_c) of various carbon materials and the relation between structures of carbon materials and its electrochemical properties were discussed in the previous study [11]. Polyvinylidene difluoride (PVDF) is a better binder than ethylene/propylene/diene polymer (EPDM) for carbon electrode materials, and the electrolyte ($LiPF_6$ dissoved in (EC + DEC)) is adequate for the lithium cell [12,13]. In this study, the relation between the structure of the carbon materials and their electrochemical properties in this lithium ion cell system was examined.

2. Experimental

Artificial graphite (IG-11, SGP-25 and Nippon carbon CB-400), carbon black, activated carbon and mesophase carbon microbead were heat-treated graphitized under a reduction atmosphere at 600°C, 2000°C, 2200°C, 2300°C, 2400°C and 2500°C in order to study the graphitizating process and to obtain carbon materials with a various degree of graphitization. The microstructure of carbon materials were characterized by X-ray diffraction (XRD) and refined with the Rietveld method. The experimental diffraction pattern was fitted with a calculated profile using a crystal structure model.

* Corresponding author. Tel.: +886-2-3925301; fax: +886-2-3925301.

0254-0584/98/$19.00
PII S0254-0584(98)00003-0

After Rietveld analysis, the crystal parameters were identified and the graphitization degree and its crystalline sizes (L_a and L_c) were calculated. The carbon anodic electrodes were prepared by wet mixing of carbon materials, binder (PVDF) and solvent (n-methyl-2-pyrrolidone) and the carbon slurry was then spread on the nickel sheet. A typical three-electrode cell was constructed for electrochemical measurements. The carbon materials are used as working electrodes and an Li metal foil is used for both the counter and reference electrodes. The electrochemical behaviors of the carbon materials were investigated by using the cyclic voltammetry with a different sweep rate in a 1 M $LiPF_6$ solution of a 50:50 (volume) mixture of ethylene carbonate (EC) and diethylene carbonate (DEC). The interfacial properties at carbon/electrolyte solution were studied by electrochemical impedance spectroscopy (EIS900) with a frequency range of 100 KHz to 0.1 Hz. A two-electrode cell was constructed with carbon and lithium metal foil for capacity testing in the same electrolyte solution. These cells were cycled at 0.223 mA cm^{-2} and 0.01–3.0 V cut-off voltages for charge and discharge.

3. Results and discussion

The electrochemical behavior of the composites, which involved mixing graphite with montmorillonite and TEF oligmer, is very complicated in this experiment. It is becoming more difficult to analyze the electrochemical properties of the composite electrode. It requires more work to be done in the future. The purpose of this report is to discuss the electrochemical properties of various carbon materials electrode.

In a previous study [11], the XRD patterns should be refined using the Rietveld method which can modify the peak profile, zero shift and orientation to obtain the exact crystal parameters. Although the Franklin equation is generally used to calculate the graphitization degree, the Maire and Mering equation was much better in this case. We also found that there exists the rhombohedral graphite phase with about 20% in the artificial graphite. The data, analyzed using the Rietveld method with a two-phase model (hexagonal and rhombohedral), gives a much better fit than that for one phase [11].

It is observed that the graphitized process of the carbon begins at 2000°C. Although the carbon black and activated carbon are the non-graphitization carbon materials, similarly to the graphite materials, their degree of graphitization increases as the temperature increases and changes linearly with a relation. The crystallite size (L_c) of graphite material is largest (350 ~ 605 Å) in these carbons and rising as the $d(002)$ increases. The L_c of carbon black and activated carbon are middle (20–30 Å) and smallest (15–35 Å), respectively, and rising as the $d(002)$ decreases. The L_a is also in the same distribution.

Typically, the anodic and cathodic peaks in the cyclic voltammetry of graphite powder occur at 0–1.1 V versus Li/Li+. With the increase in the potential sweep rate (ν in mV min^{-1}), the anodic peak shifts to a higher potential and shows a larger current. In the previous study [11], the anodic potential changes linearly with sweep rate and it can be separated into two sections. As described as the Randles–Sevcik equation [14], the anodic and cathodic current increase as $\nu^{1/2}$. At lower ν (< 12 mV min^{-1}), the relationship between anodic current and $\nu^{1/2}$ shows a straight line which passes through the origin point, which can be described as the Randles–Sevcik equation. As ν (< 12 mV min^{-1}) increases, the anodic currents are lower and tend to level off. According to the reversible reaction, $xLi^+ + xe^- + 6C \Leftrightarrow Li_xC_6$, where $x = 0$–1, the anodic current is caused by lithium deintercalation.

The typical charge–discharge curve for the graphite electrode is shown in Fig. 1. The Coulombic efficiency at the first cycle of various graphite materials is about 80%. There is a voltage plateau from 0.8 to 0.6 V at the first cycle due to the surface film growth for the typical graphite electrode, but this is not found at the subsequent charge–discharge curves. The same behavior was obtained from the difference between the first cycle profile with a cathodic peak near 0.7 V and the next one of the cyclic voltammetry test pattern. The surface film capacity loss is the most serious energy loss for lithium ion batteries with a graphite electrode. It is also observed that a small amount of electrical quantity was consumed from the open circuit voltage (OCV; 3.0–3.3 V) to 0.8 V which may be caused by electrolyte decomposition. The reversible capacity occurs from 0.25 to near 0 V of charge–discharge profile. The capacity loss of different graphite electrodes is shown in Fig. 2. Generally, it was considered that the irreversible capacity loss of those graphite electrodes was completely caused by the surface film growth. From Fig. 2 one can find that the surface film loss of IG-11 and MCMB is larger than SGP-25 and Nippon Carbon CB-400. The first cycle discharge capacity of various graphite materials with a

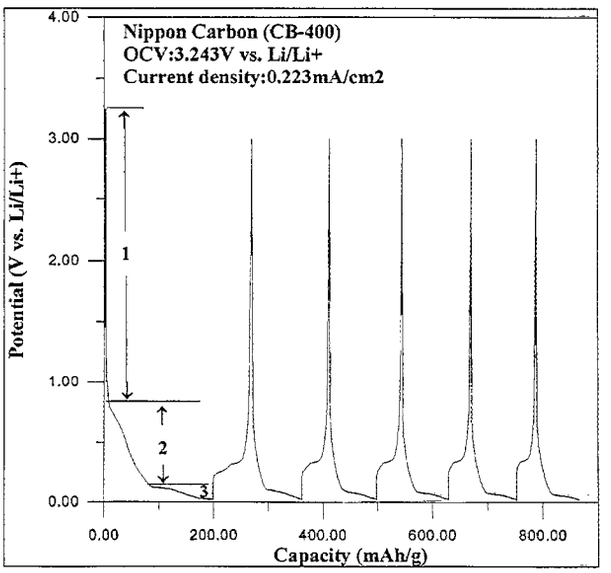

Fig. 1. Charge–discharge curves of typical graphite from a three-electrode cell with an Li metal counter electrode and 1 M LiPF6/Ec + DEC, cycled at 0.223 mA cm^{-2}, cut-off votages of 0.01 ~ 3.0 V.

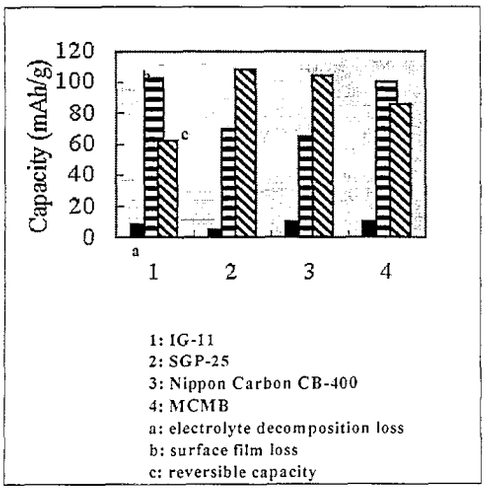

Fig. 2. The irreversible capacity loss and reversible capacity of different graphite electrodes at first cycle.

different degree of graphitization is shown in Fig. 3. It is shown that as the degree of graphitization rises, the discharge capacity increases for graphite and decreases for non-graphitized carbon such as carbon black and activated carbon. In fact, similarly, with the increase of crystallite size (L_c), the discharge capacity of graphite increases and that of carbon black and activated carbon decreases.

A typical Nyquist diagram, shown in Fig. 4(a), is composed of two semicircles and a Warburg branch at low frequency. The semicircle obtained at intermediary frequencies was associated with the charge transfer impedance and the high frequency semicircle to the passivation film. Because the frequency of the test instrument is limited to 0.1 Hz, the Warburg branch is not clearly observed at low frequency from a fresh cell with the Nippon Carbon CB-400 electrode. In the liquid electrolyte, after cyclic voltammetry or the charge/discharge test, the reduction yields a film that protects the lithiated carbon from direct contact with the electrolyte. The resistance of the cell with graphite electrodes increases after examination, the Warburg branch became larger than that with fresh graphite electrode, as observed in Fig. 4(b). We analyzed the experimental data used a EIS900 electrochemical impedance system by an equivalent circuit model, as shown in Fig. 4(a).

The composition of the total resistance of this system included the sum of the resistance of the electrolyte and the current collector (R_e), the charge transfer resistance (R_{CT}) and the film resistance (R_{film}). This indicates that the semicircle in the middle frequency region and the Warburg branch in the low frequency region correspond to the impedance for the graphite/electrolyte interfacial process and lithium diffusion into the graphite layer, respectively.

4. Conclusions

The exact degree of graphitization and crystallite sizes (L_c and L_a) of graphitized carbon and non-graphitized carbon

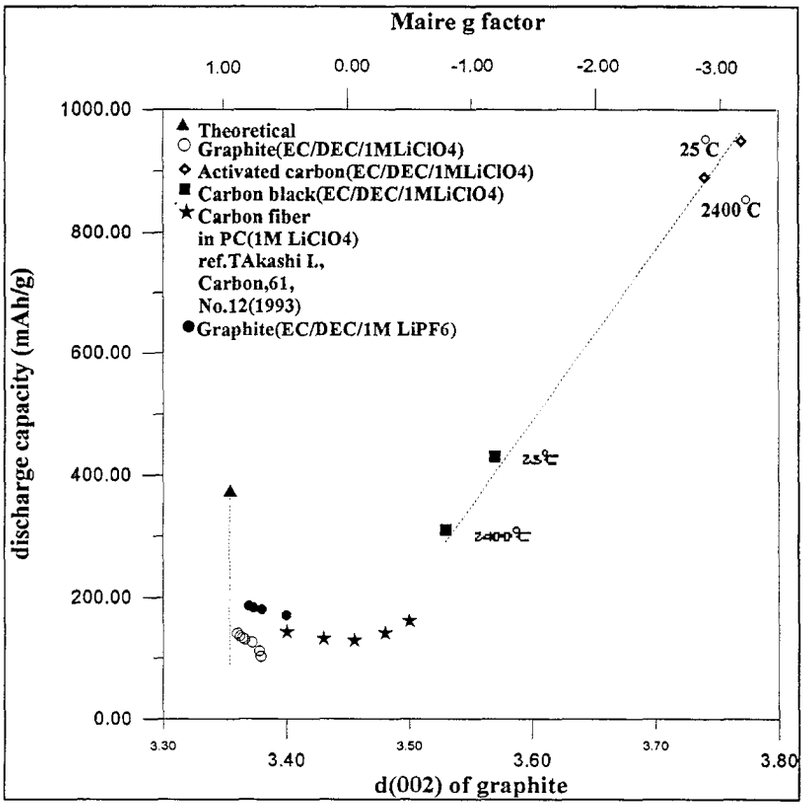

Fig. 3. The relationship between first cycle discharge capacity and different graphitization degree of various carbon materials.

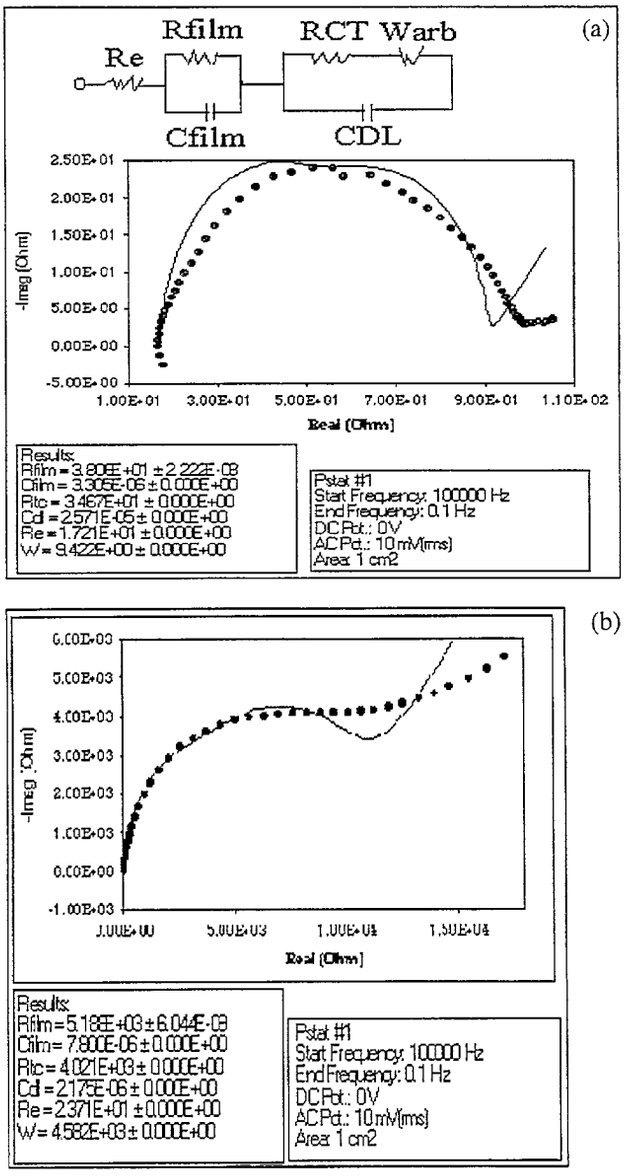

Fig. 4. (a) The impedance spectrum of the Nippon Carbon CB-400 electrode in LiPF6/(EC + DEC) and equivalent circuits. (b) The impedance spectrum of Nippon Carbon CB-400 electrode after a cyclic voltammery test.

can be obtained by XRD and Rietveld analysis with a hexagonal structure model.

The anodic and cathodic peaks of various carbon materials existed by using the cyclic voltammetry method with different potential sweep rates. This might be attributed to the inter/deintercalating behaviors of lithium ions. Besides, the anodic current shows a reversible behavior at a lower potential sweep rate of below 12 mV min^{-1}.

The irreversible capacity loss for various graphite materials consists of the loss owing to the formation of the surface film, electrolyte decomposition and unknown loss capacity that occurs in the range of lithium ion intercalating voltage. It is suggested that the irreversible capacity losses would be decreased by selecting the graphite materials with a high degree of graphitization and microcrystals.

As the degree of graphitization increases and crystallite sizes increase (L_c and L_a), the capacity increases for graphite and decreases for non-graphitized carbon including carbon black and activated carbon.

The semicircle in the middle frequency region dependence of the impedance for the graphite/electrode interfacial process and the Warburg branch is indicated by the behavior of the lithium diffusion in the graphite layer.

References

[1] T. Saito, T. Nohma, M. Takahashi, M. FuJimoto, K. Nishio, Proceedings of the 183rd Meeting of the Electrochemical Society, Abstr. No. 40, 1993.
[2] R. Fong, U. von Sacken, J.R. Dahn, J. Electrochem. Soc. 137 (1990) 2009.
[3] O. Chusid, Y.E. Ely, D. Aubach, M. Babai, Y. Carmeli, J. Power Sources 43–44 (1993) 47.
[4] H.X. Yang, X.P. Ai, M. Lei, S.X. Li, J. Power Sources 43-44 (1993) 399.
[5] J.R. Dahn, R. Fong, M.J. Spoon, Phys. Rev. B 42 (1990) 6424.
[6] M. Endo, J.I. Nakamura, Y. Sasabe, T. Takahashi, M. Inagaki, TANSO 165 (1994) 282.
[7] K. Tatsumi, A. Mabuchi, N. Iwashita, H. Shioyama, H. Fujimoto, S. Higuchi, Proceedings 183rd Meeting of the Electrochemical Society, 1993, p. 224.
[8] T. Nagaura, 4th International Rechargeable Battery Seminar, Deerfield Beach, FL, 1990.
[9] N. Imanishi, et al., J. Electrochem. Soc. 140 (1993) 315.
[10] J.O. Besengard, et al., J. Power Sources 43-44 (1993) 693.
[11] Y.H. Lee, J.R. Tarng, K.M. Lin, G.H. Chen, W.K. Chang, in: R.Y. Lin, Y.A. Chang, R.G. Reddy, C.T. Liu (Eds.), Design Fundamentals of High Temperature Composites, Intermetallics, and Metal–Ceramics Systems, TMS, 1995, p. 385.
[12] O. Chusid, Y. Ein Ely, D. Aurbach, J. Power Sources 43 (1993) 47.
[13] Shoichiro Mori, Hitoshi Asahina, Hitoshi Suzuki, Ayako Yonei, Eiki Yasukawa, 8th International Meeting on Lithium Batteries, 1996, pp. 41–43.
[14] P.T. Kissinger, W.R. Heineman, J. Chem. Educ. 60 (1983) 702.